



## Supporting Online Material for

### **Generation of Spatial Patterns Through Cell Polarity Switching**

Sarah Robinson, Pierre Barbier de Reuille, Jordi Chan, Dominique Bergmann,  
Przemyslaw Prusinkiewicz, Enrico Coen\*

\*To whom correspondence should be addressed. E-mail: [enrico.coen@bbsrc.ac.uk](mailto:enrico.coen@bbsrc.ac.uk)

Published 9 September 2011, *Science* **333**, 1436 (2011)  
DOI: 10.1126/science.1202185

#### **This PDF file includes:**

Materials and Methods  
Figs. S1 to S10  
References

## Materials and methods

### Plant material

The following fluorescent marker lines were used for tracking: Ltl6b (26), BASL::GFP BASL; pm-rb (27) (11), SPCH::SPCH-GFP (4) crossed to PIN3::GFP (4). Seeds were sterilised with 70% ethanol containing 0.05% SDS (SODIUM DODECYL SULFATE) for 10 min and then rinsed with 100% ethanol. Plants were grown on MS agar medium [0.9% (w/v) agar, 1× Murashige and Skoog salt mixture (28), 0.5mg/ml MES (4-Morpholineethanesulfonic acid), pH 5.7] with 1% (w/v) glucose. Seeds were kept at 4°C in the dark for 2 days (stratification) before being transferred to the growth room, where they were placed upright (20°C, 16hour light per day).

### Imaging

Seedlings were transferred to a perfusion chamber for imaging chamber was perfused with ¼ strength liquid MS growth media (as above) (pH 5.8), with 0.75% (w/v) sucrose, at a rate of 1µl/s. The Ltl6b, line was imaged starting 5 days after stratification while the other lines were imaged from 7 days after stratification. Images were taken with a Zeiss LSM 5 EXCITER at intervals of between 2 and 12 hours. The raw images were converted to single (png) slices using the bioformats convertor (29). Images were processed using ImageJ despeckle or median filter with 2px threshold. Some images were further processed using a rolling ball background subtraction (30). A surface projection was made from the z-stacks using Merryproj (31). The cell areas were measured in ImageJ using the original cell outline. Analysis of cells at the very edge of the leaf was avoided to prevent potential errors from the curvature of the leaf. For modelling the placement of peripheral BASL away from new walls, cell outlines were digitised by placing points along the walls. For modelling the generation of cell arrangements from individual lineages (Fig. S12) only cell vertices present in the initial cell were used. Their location in subsequent timepoints was recorded and used to determine displacements through growth. Cell edges were approximated as straight lines.

### Modelling

Models were created using the VVe modelling environment which is an extension of the VV systems (32). (Models are available on request). To consider particular cell lineages vertices were displaced over time by linearly interpolating between positions observed at particular time points. For more general parameter searches, vertices

were displaced according to a growth tensor  $\begin{bmatrix} K_{max} & 0 \\ 0 & K_{min} \end{bmatrix}$  where  $K_{max}$  and  $K_{min}$  are the maximal and minimal

relative rates of growth, respectively (i.e.  $K_{min} < K_{max}$ ). Only the cell with SPCH was permitted to divide and the model was stopped when the SPCH cell was internalised. In the final model, peripheral BASL was localised at a position that minimises its inverse distance from points along the new division boundary. Formally, at each point  $p$  on the periphery of the cell, we evaluate a weight function  $w$ :

$$w(p) = \int_0^L \frac{\delta(s(x))}{d(p, s(x))} dx$$

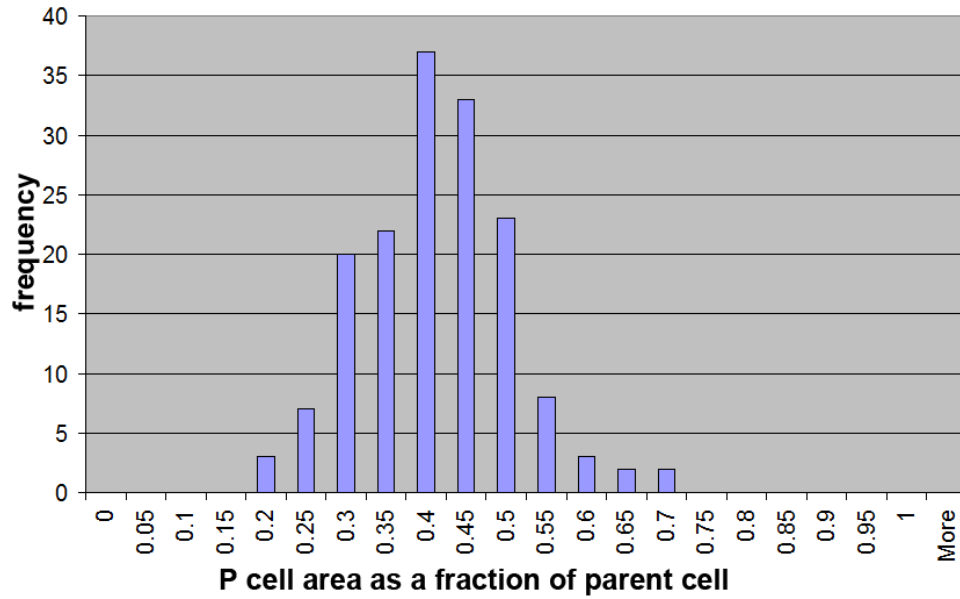
where  $L$  is the perimeter of the cell,  $s$  is an arc-length parametric function for the contour of the cell,  $\delta$  is a function identifying the recent walls (i.e. its value is 1 on the cell walls formed since the lineage acquired P cell fate, 0 everywhere else, or for the one wall model only the latest wall has a value of 1), and  $d(p, s(x))$  is the distance from point  $p$  to point  $s(x)$ . The integral was approximated using the rectangle (or mid-point) method with 100 rectangles per side of the cell. Peripheral BASL is drawn as a line for display purposes.

The model has four parameters: the initial placement of peripheral BASL, the cell shape (i.e. the ratio length on width), the cell growth (i.e. the ratio  $K_{min}$  on  $K_{max}$ ) and the amount of nuclear displacement. Many different parameter combinations can produce the same result. Examples of the parameters that give the patterns are given. The displacement of the nucleus was along the vector defined by the position of peripheral BASL and the cell centre. The displacement is a percentage of the distance from the centre of the cell to the cell boundary. Fig. 3F and Fig. 3G use the same model parameters with an initial shape that is almost square (50 by 52 pixels), a nuclear movement of 32% and a growth anisotropy of 0.5. Fig. 3F used only the most recent division wall to compute the new location of peripheral BASL while Fig. 3G used all of the new walls as shown in the equation above.

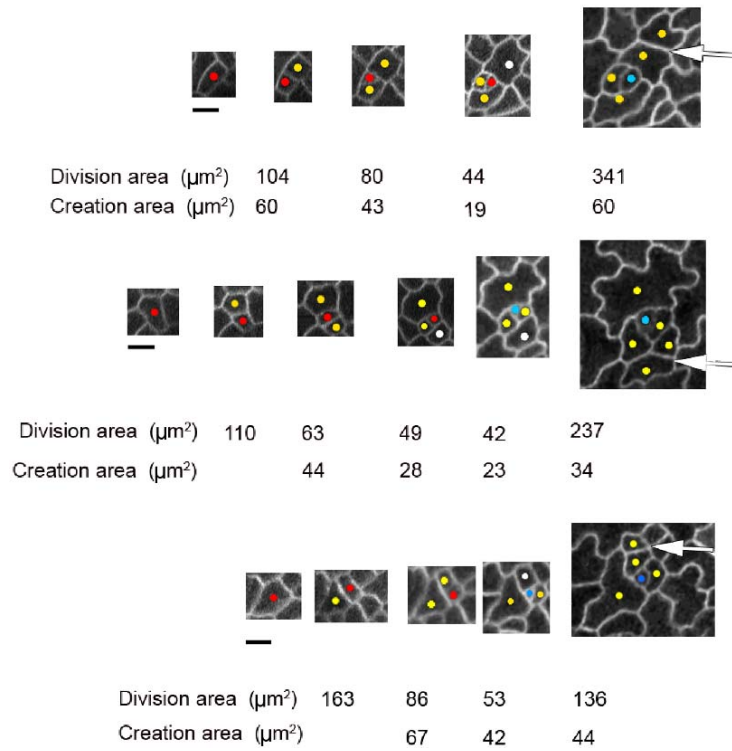
Fig. 4A was generated using an isotropy of 1, a shape that is 2.4 times as long in the  $x$  direction as the  $y$  direction and has a nuclear displacement of 40%, a wide range of parameters produce this shape. Fig. 4B was generated starting from a shape that is 2.5 times as long in the  $x$  direction compared to  $y$ , has a growth anisotropy of 0.8 and a nuclear displacement of 40%. Fewer parameter combinations result in this shape. An aspect ratio of 1, an isotropy of 0.6 and 32% nuclear displacement can be used to generate a shape equivalent to that seen in Fig.3G with the same start shape used in Fig. 4. Modelling of individual lineages requires two parameters which were varied to produce the best fit to the data. The timing of subsequent cell divisions (division area as a ratio of birth size) and the amount of nuclear movement (as a percentage of the maximum possible distance from the centre along the vector defined by the vector of BASL location and the cell centre) Parameters in this order for Fig 4 are: (E) 1.6,

48%, (H) 1.1, 22% and (K) 1.5, 50%. The birth size of the original cell is not known so the timing of the first division is roughly the observed time of division.

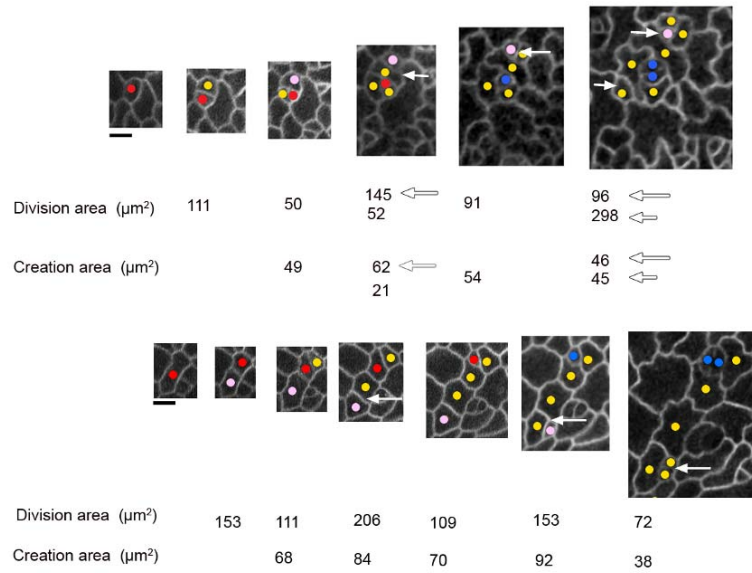
**Supplementary figures**



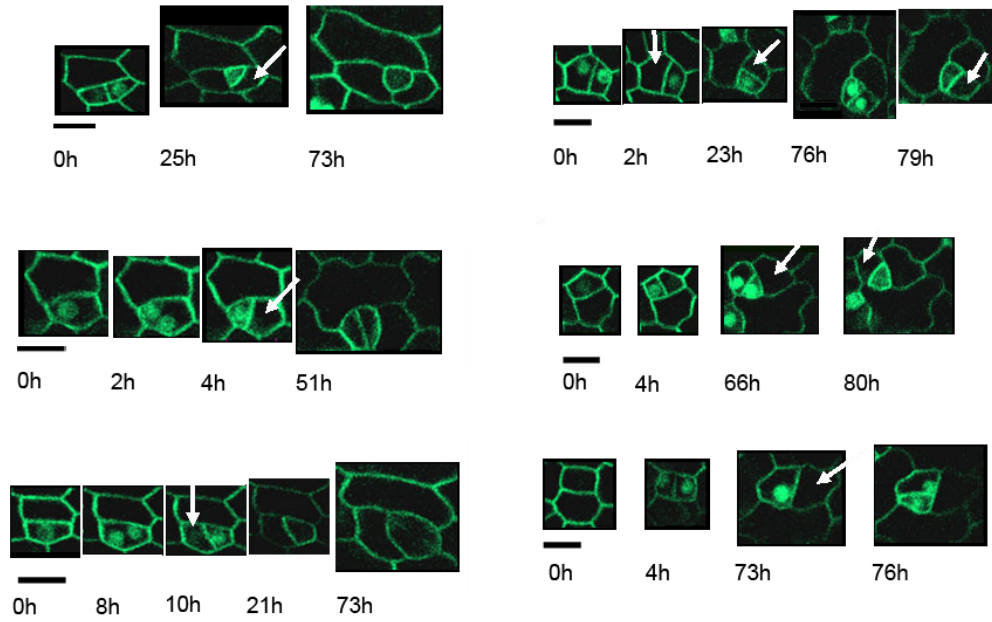
**Fig. S1.** The area of both daughter cells was measured at the time of divisions. The area of the P cell daughter was found as a percentage of the sum of the daughter cell areas. The P cell is usually smaller (less than 50% of the parent. On average the P cell daughter is 39% of the parent area (based on 163 divisions of tracked P cells). The areas were measured using ImageJ on the surface projections of the leaf produced by Merryproj.



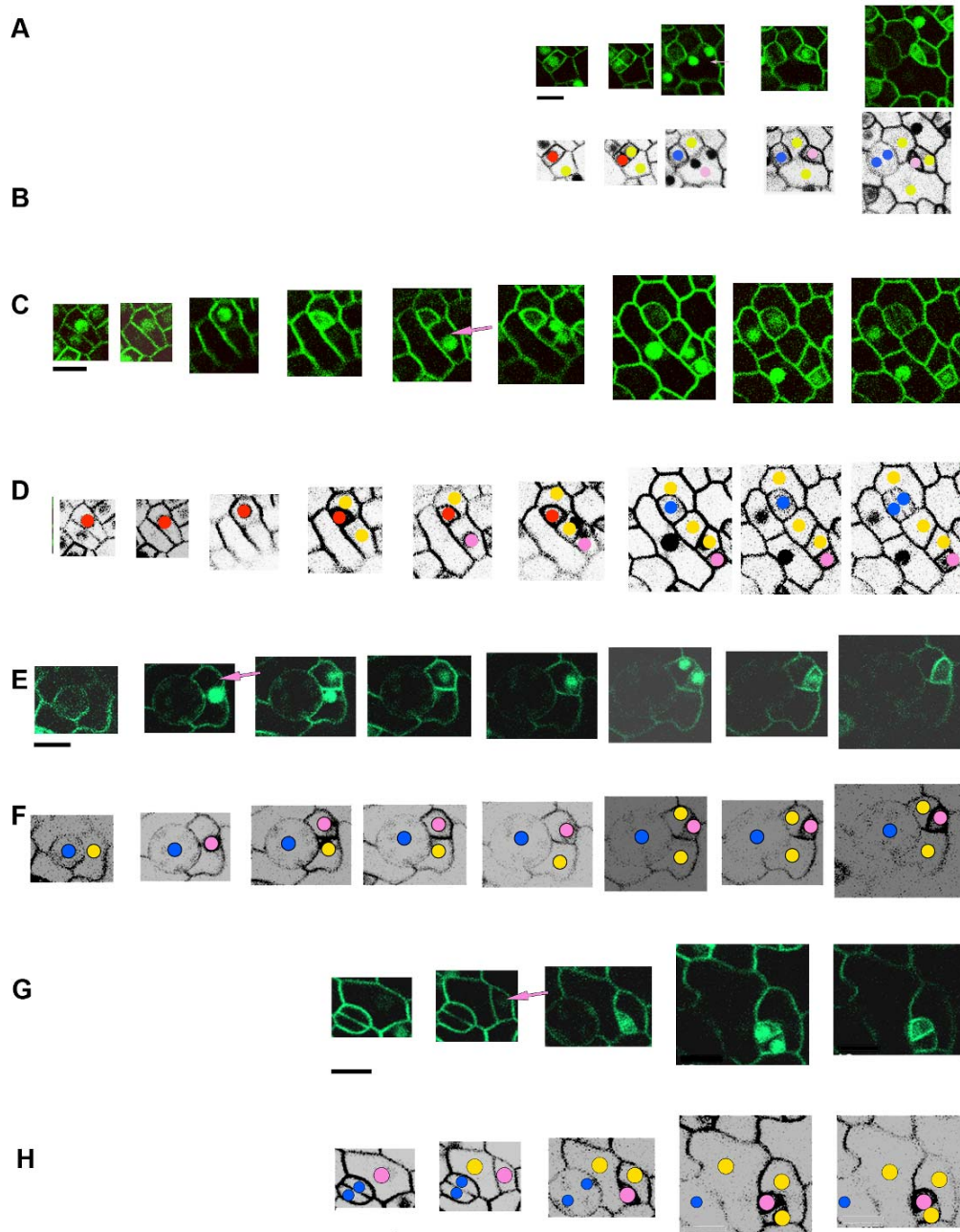
**Fig. S2.** Some N cells divide (arrow). N cells take longer to divide than P cells dividing only once in the time it takes P cells to make 2-3 divisions. The N cells are large when they divide and tend to divide at more than twice their birth size (creation area). Division and creation areas refer to P cells, except for the rightmost numbers which refer to N cells. Scale bar (black line) is  $10\mu\text{m}$ .



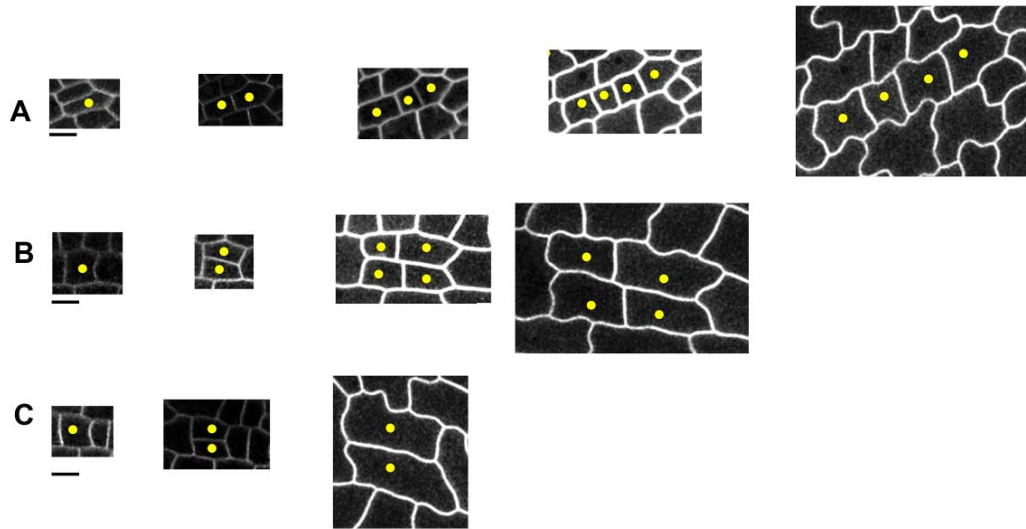
**Fig. S3.** Some N cells produced as a result of the division of a P cell regain P cell fate and undergo many divisions (arrow). When two divisions happen in the same interval, they are distinguished by arrow size. Divisions of P cells are not marked with arrows. Scale bar (black line) is 10 $\mu\text{m}$ .



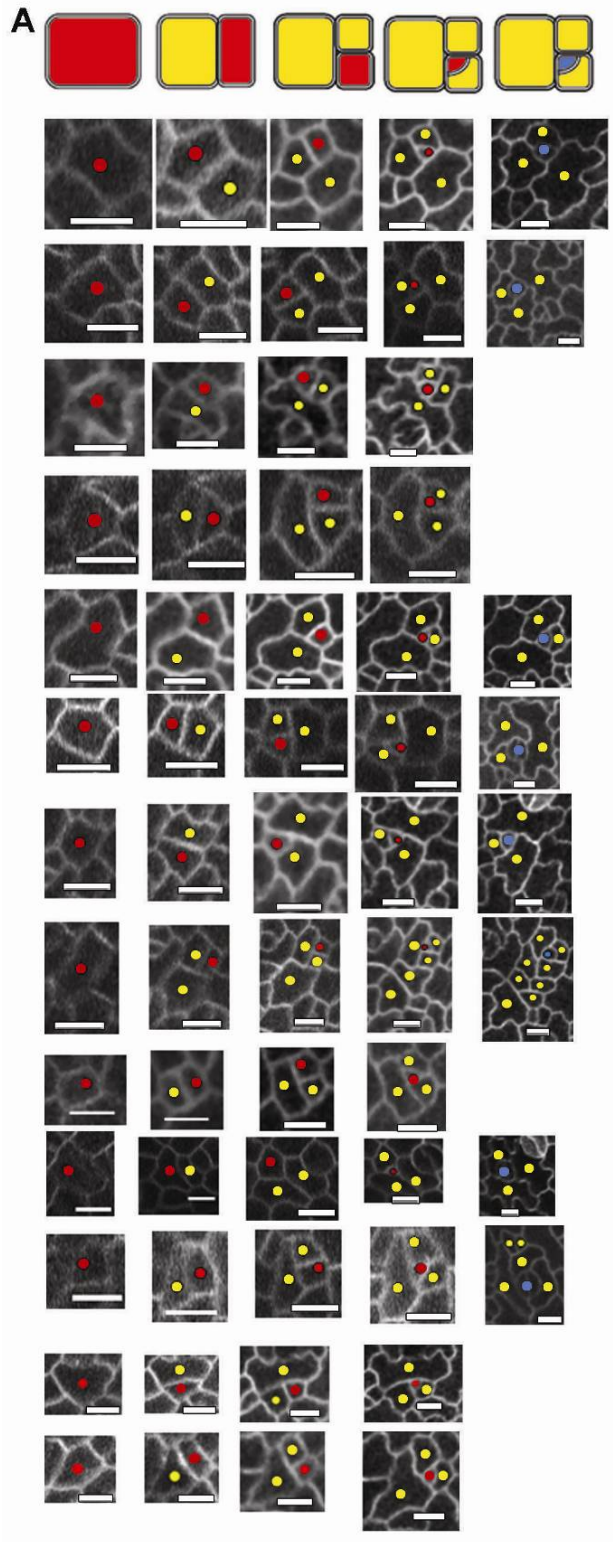
**Fig. S4.** Tracking GFP-labelled SPCH protein shows that SPCH signal disappears in N daughter cells (white arrows) a few hours after division. The cell that maintains SPCH expression has P cell properties and continues to divide until a GMC is formed. Image times are shown underneath the images. Times are shown to the nearest hour. Scale bar (black line) is 10 $\mu$ m.

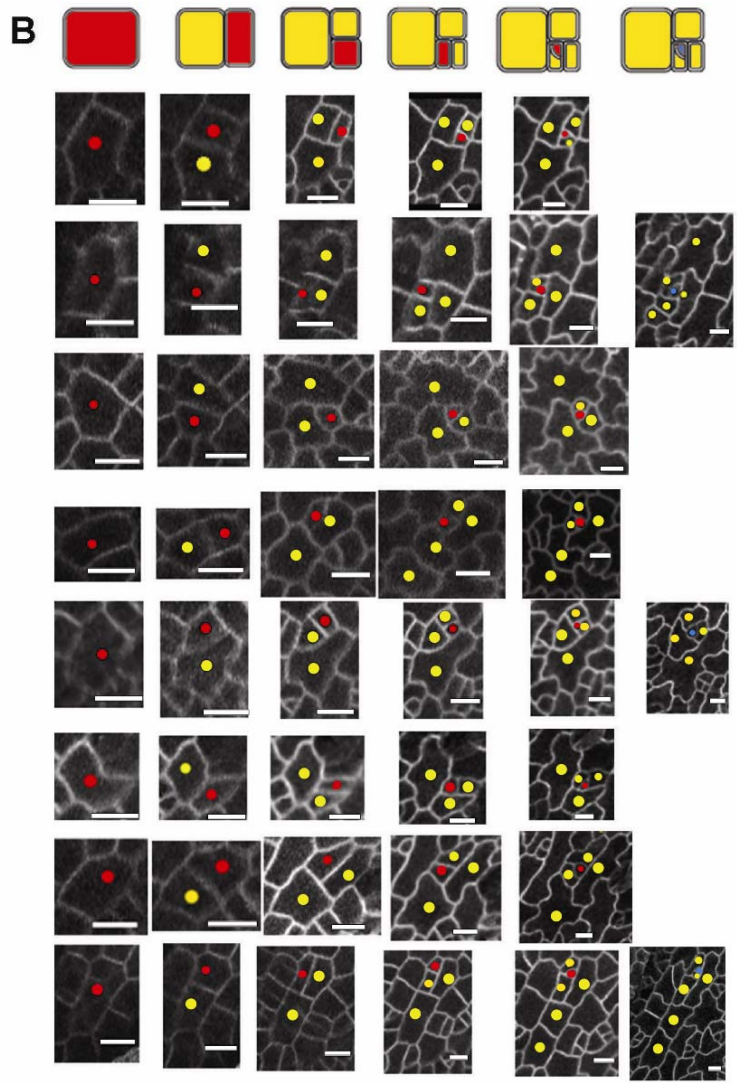


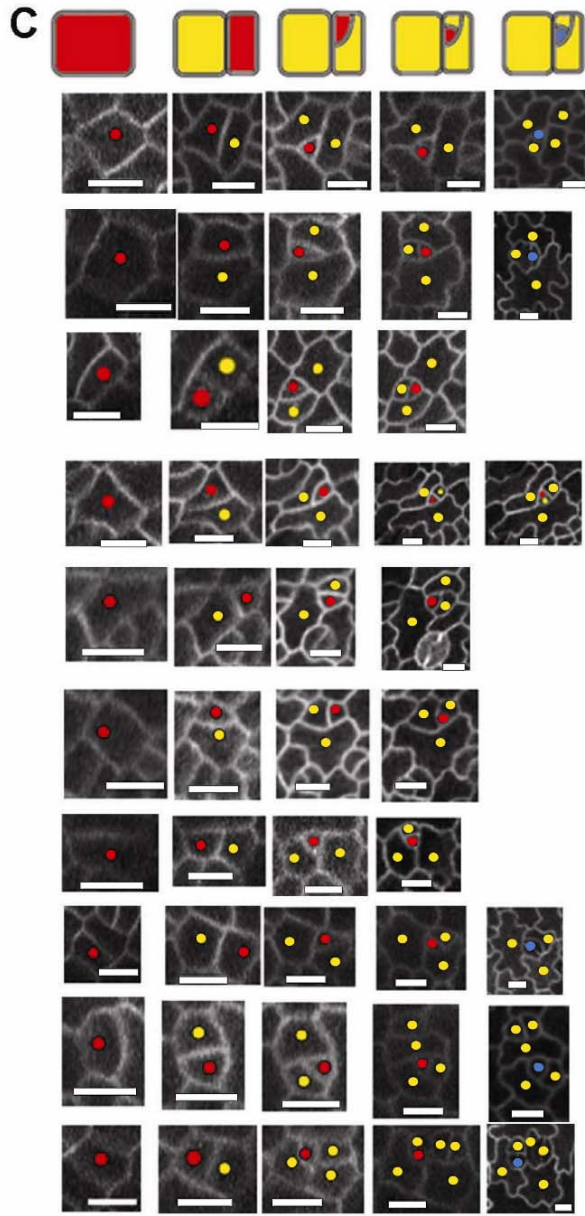
**Fig. S5.** (A-C) Tracking GFP-labelled SPCH protein in further lineages shows that N cells which regain P cell fate also re-gain SPCH (pink arrows). SPCH is then inherited by the P cell daughter as shown in FIG. 2S. (A) The initial division of the cell which has regained SPCH (pink) occurs at  $162 \mu\text{m}^2$  which is almost 5 times its birth size of  $34 \mu\text{m}^2$ . (B) The initial division occurs at  $90 \mu\text{m}^2$ , one daughter divides again at  $73 \mu\text{m}^2$  which is less than twice its birth size of  $45 \mu\text{m}^2$ . (C) Imaging at later stages shows cells flanking mature stomata can re-gain SPCH and divide to produce a secondary meristemoid. The first division is at  $123 \mu\text{m}^2$ . The cell subsequently divides at  $73 \mu\text{m}^2$ , less than twice the birth size of  $53 \mu\text{m}^2$ . Image times to the nearest hour (A) (00h, 04h, 23h, 28h, 50h). (C) (00h00, 02h, 11h, 26h, 30h, 32h, 50h, 52h, 54h), (E) (00h, 26h, 29h, 36h, 44h, 48h, 51h, 58h). (G) (00h, 2h, 23h, 49h, 52h). Scale bar (black line) is  $10 \mu\text{m}$ .



**Fig. S6. (A-C)** Tracking of the *spch* mutant shows bifurcating lineages. There are fewer cell divisions and at larger sizes, similar to that seen in N cell populations. **(A)** The cell on the left divides at  $176 \mu\text{m}^2$ , producing daughter of size  $101 \mu\text{m}^2$  and  $76 \mu\text{m}^2$ . The larger daughter divides at  $179 \mu\text{m}^2$  16h later, and the smaller daughter divides at  $194 \mu\text{m}^2$ , 12h later. There are no further divisions in the remaining 31h that the lineage was followed for. **(B)** The cell on the left divides at  $188 \mu\text{m}^2$  producing two daughters of equal size which both divide 39h hours later at sizes of  $326 \mu\text{m}^2$  and  $298 \mu\text{m}^2$  and do not divide again. **(C)** The cell on the left divides only once in the 80 hour period of imaging at a size of  $181 \mu\text{m}^2$  producing daughters of size  $81 \mu\text{m}^2$  and  $100 \mu\text{m}^2$ . Scale bar (black line) is  $10\mu\text{m}$ . Image times are to the nearest hour.







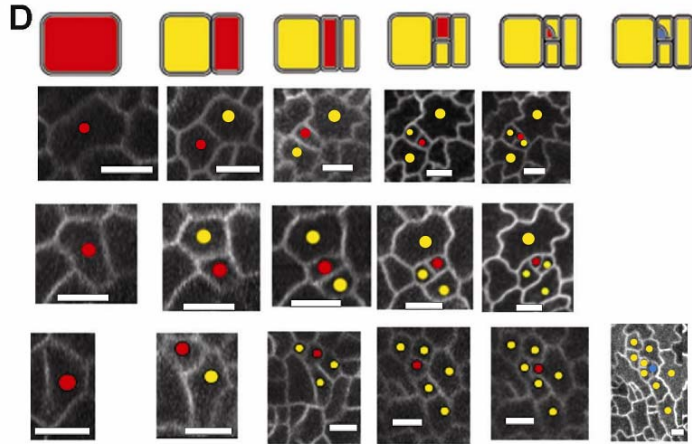


**Fig. S7.** Patterns observed among lineages which internalised the GMC (34/50). Interpretive diagrams (A,B,C,D) are shown above time-lapse confocal images. The division of N cells is not considered when classifying the lineages. (A-B) The P cell undergoes 2-3 divisions in alternating orientations, followed by a division across adjacent walls (21 lineages). The result is a spiral arrangement. (C) As A except that two successive divisions span adjacent walls (10 lineages) (D) Two parallel divisions prior to an alternating division and then a final division that joins adjacent walls (3 lineages). Extra divisions captured are not shown for simplicity. Scale bars (white lines) are 10 $\mu$ m.

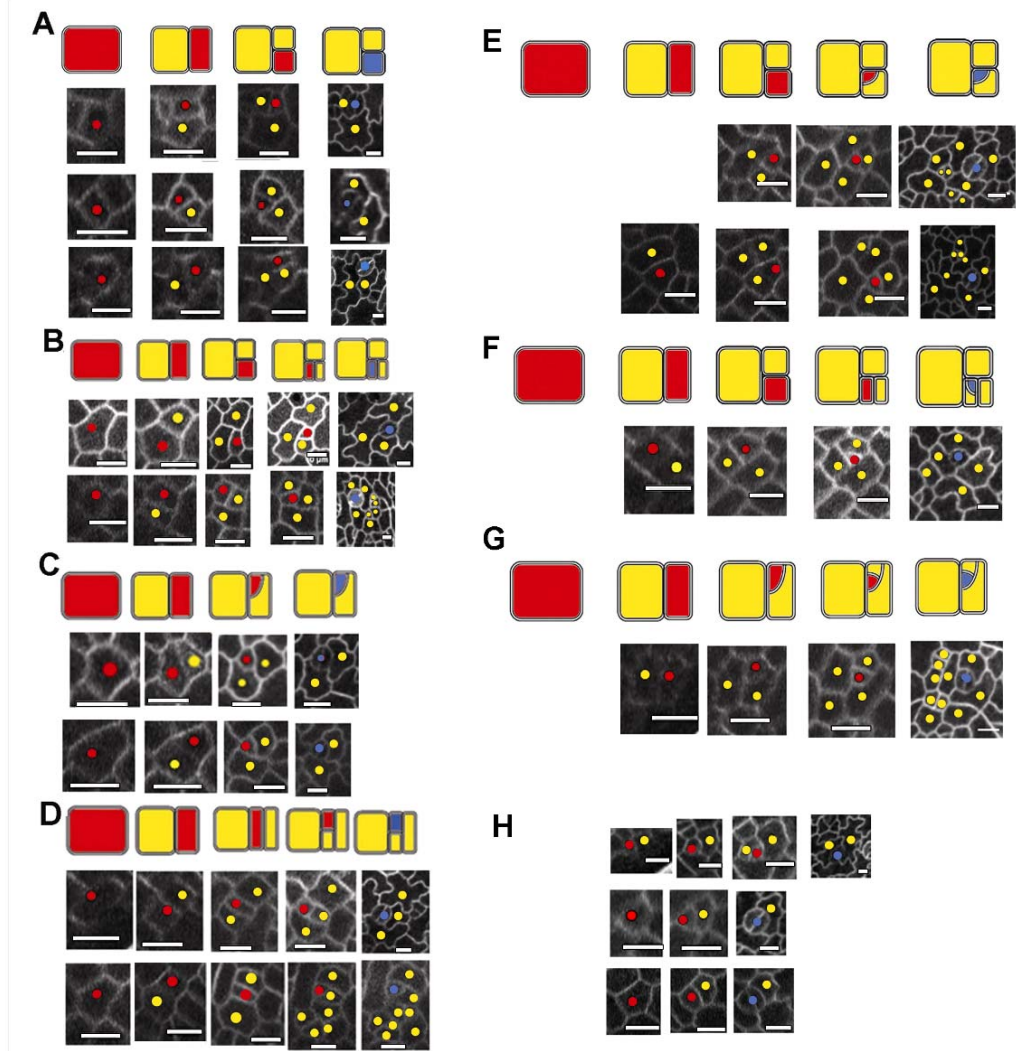


**Fig. S8.** Patterns observed among lineages which did not internalise the GMC (16/50). Interpretive diagrams (**A-G**) are shown above time-lapse confocal images. (**A-D**) The P cell becomes a GMC before it is internalised. These lineages are truncated versions of the patterns in Fig. S2. (**A-B**) Truncated versions of pattern Fig.S2 A-B. The P cell undergoes 2-3 divisions in alternating orientations, but does not have a final division across adjacent walls (3 lineages). (**C**) Truncated versions of pattern Fig.S2C. (2 lineages). (**D**) Truncated versions of pattern Fig.S2C. (2 lineages). (**E-G**) Lineages in which initial divisions were not captured but the final arrangement is consistent with the patterns identified. (**E**) is consistent with **A**, (**F**) with **B** and (**G**) with **C**. (**H**) In 3 lineages 2 or fewer divisions were observed and their arrangement could not be classified. Scale bars (white lines) are 10 $\mu$ m.

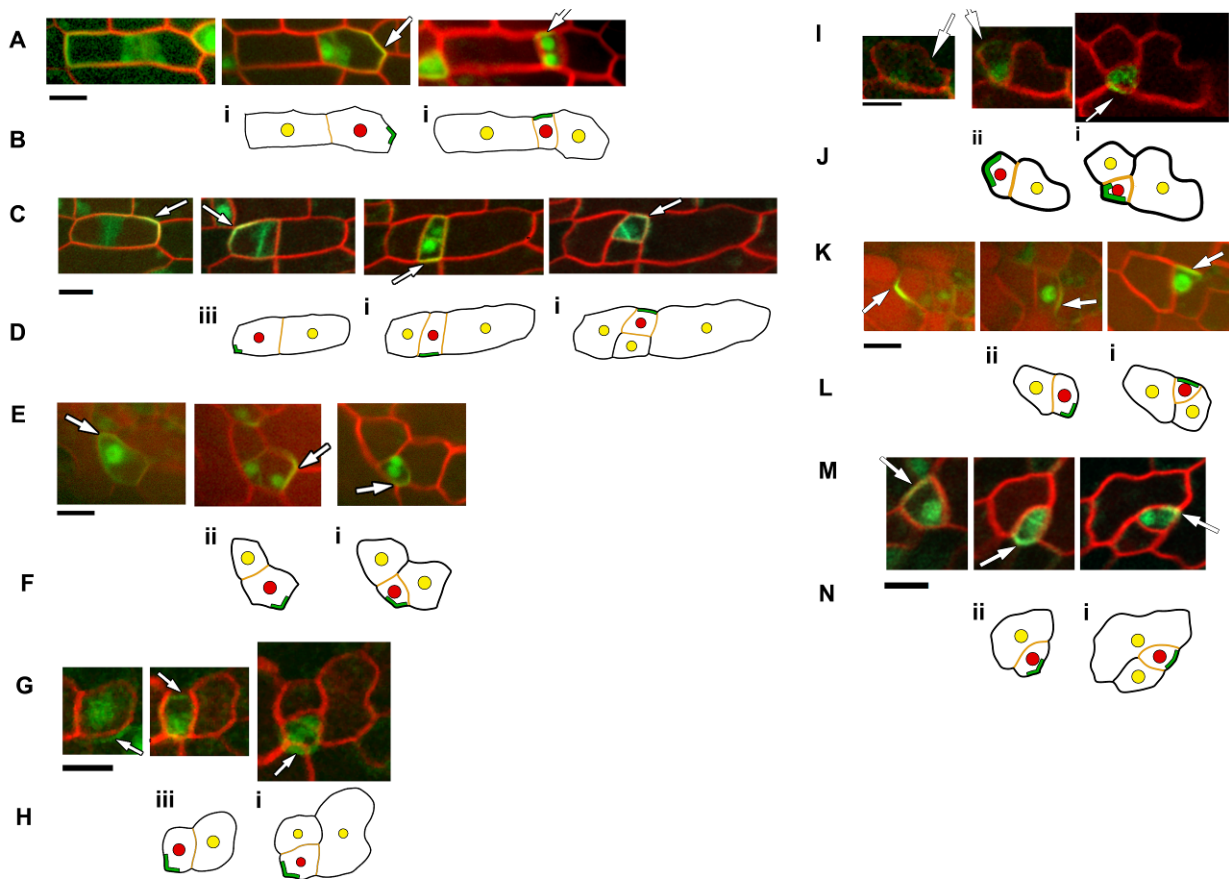


**Fig. S9.** Comparing the location of peripheral BASL to that predicted by the model. Confocal images show cells expressing GFP-labelled BASL protein (green) and a plasma membrane marker (red) followed for multiple rounds of division. Digitised outlines beneath each image sequence highlight cell walls (black) and new division walls (orange) around the P cell. The predicted position of peripheral BASL (green line) is the region furthest from new division walls, with the centre of the region computed using the formula for the weight function,  $w(p)$ , described in the methods. Out of 21 divisions analysed, 13 cases (labelled i here and in Fig. 4) showed good agreement between the observed position of peripheral BASL and that predicted by the model. In 5 cases the predicted and observed BASL positions were slightly discordant (labelled ii here and in Fig.4). In the remaining 3 cases, peripheral BASL was located at the opposite end to that predicted (labelled iii here and in Fig.4) due to cell symmetry.



**Fig. S10.** Modelling observed cell lineages. Confocal images of tracked lineages are shown above corresponding model outputs. The images were used to define the initial geometry, initial location of peripheral BASL and displacement of the initial vertices to simulate an entire stomatal lineage. The model was used to predict both the placement of division walls and placement of peripheral BASL. The ratio of division and amount of nuclear displacement were varied from one lineage model to the next to achieve the best fit but remained fixed for all the divisions of the lineage. The model could account for all three patterns of stomata divisions observed: (A, B) patterns corresponding to Fig. 2E, (C,D) patterns corresponding to Fig. 2C, (E-G) patterns corresponding to Fig. 2A. For some divisions (labelled iii), predicted peripheral BASL is located opposite to the position observed, most likely because of cell symmetry, leading to the lineage spiralling in the opposite direction to that observed. The simplicity of the model also results in division walls being placed slightly differently which can result in incorrect placement of peripheral BASL.

## References and Notes

1. T. Sachs, *Pattern Formation in Plant Tissues*, P. W. Barlow, D. Bray, P. B. Geen, J. M. W. Slack, Eds. (Developmental and Cell Biology Series, Cambridge Univ. Press, Cambridge, 1991).
2. M. K. Barton, Making holes in leaves: Promoting cell state transitions in stomatal development. *Plant Cell* **19**, 1140 (2007). [doi:10.1105/tpc.107.051177](https://doi.org/10.1105/tpc.107.051177) [Medline](#)
3. M. Geisler, J. Nadeau, F. D. Sack, Oriented asymmetric divisions that generate the stomatal spacing pattern in arabidopsis are disrupted by the too many mouths mutation. *Plant Cell* **12**, 2075 (2000). [Medline](#)
4. C. A. MacAlister, K. Ohashi-Ito, D. C. Bergmann, Transcription factor control of asymmetric cell divisions that establish the stomatal lineage. *Nature* **445**, 537 (2007). [doi:10.1038/nature05491](https://doi.org/10.1038/nature05491) [Medline](#)
5. G. R. Lampard, C. A. Macalister, D. C. Bergmann, *Arabidopsis* stomatal initiation is controlled by MAPK-mediated regulation of the bHLH SPEECHLESS. *Science* **322**, 1113 (2008). [doi:10.1126/science.1162263](https://doi.org/10.1126/science.1162263) [Medline](#)
6. K. Ohashi-Ito, D. C. Bergmann, *Arabidopsis* FAMA controls the final proliferation/differentiation switch during stomatal development. *Plant Cell* **18**, 2493 (2006). [doi:10.1105/tpc.106.046136](https://doi.org/10.1105/tpc.106.046136) [Medline](#)
7. M. M. Kanaoka *et al.*, SCREAM/ICE1 and SCREAM2 specify three cell-state transitional steps leading to arabidopsis stomatal differentiation. *Plant Cell* **20**, 1775 (2008). [doi:10.1105/tpc.108.060848](https://doi.org/10.1105/tpc.108.060848) [Medline](#)
8. D. Bergmann, Integrating signals in stomatal development. *Curr. Opin. Plant Biol.* **7**, 26 (2004). [doi:10.1016/j.pbi.2003.10.001](https://doi.org/10.1016/j.pbi.2003.10.001)
9. L. B. Lai *et al.*, The *Arabidopsis* R2R3 MYB proteins FOUR LIPS and MYB88 restrict divisions late in the stomatal cell lineage. *Plant Cell* **17**, 2754 (2005). [doi:10.1105/tpc.105.034116](https://doi.org/10.1105/tpc.105.034116) [Medline](#)
10. L. J. Pillitteri, D. B. Sloan, N. L. Bogenschutz, K. U. Torii, Termination of asymmetric cell division and differentiation of stomata. *Nature* **445**, 501 (2007). [doi:10.1038/nature05467](https://doi.org/10.1038/nature05467) [Medline](#)
11. J. Dong, C. A. MacAlister, D. C. Bergmann, BASL controls asymmetric cell division in *Arabidopsis*. *Cell* **137**, 1320 (2009). [doi:10.1016/j.cell.2009.04.018](https://doi.org/10.1016/j.cell.2009.04.018) [Medline](#)

12. M. T. Fuller, A. C. Spradling, Male and female *Drosophila* germline stem cells: Two versions of immortality. *Science* **316**, 402 (2007).  
[doi:10.1126/science.1140861](https://doi.org/10.1126/science.1140861) [Medline](#)
13. C. van den Berg, V. Willemsen, W. Hage, P. Weisbeek, B. Scheres, Cell fate in the *Arabidopsis* root meristem determined by directional signalling. *Nature* **378**, 62 (1995). [doi:10.1038/378062a0](https://doi.org/10.1038/378062a0) [Medline](#)
14. G. J. Mitchison, M. Wilcox, Rule governing cell division in *Anabaena*. *Nature* **239**, 110 (1972). [doi:10.1038/239110a0](https://doi.org/10.1038/239110a0)
15. H. A. Harkins *et al.*, Bud8p and Bud9p, proteins that may mark the sites for bipolar budding in yeast. *Mol. Biol. Cell* **12**, 2497 (2001). [Medline](#)
16. J. E. Zahner, H. A. Harkins, J. R. Pringle, Genetic analysis of the bipolar pattern of bud site selection in the yeast *Saccharomyces cerevisiae*. *Mol. Cell. Biol.* **16**, 1857 (1996). [Medline](#)
17. P. H. J. Sahlin, H. Jönsson, A modeling study on how cell division affects properties of epithelial tissues under isotropic growth. *PLoS ONE* **5**, e11750 (2010). [doi:10.1371/journal.pone.0011750](https://doi.org/10.1371/journal.pone.0011750)
18. L. Errera, *Bot. Centralbl.* **34**, 395 (1888).
19. BASL protein becomes localized in the cell periphery at a position that minimized the inverse distance from all points along the new division boundaries. See equation in the modeling section of the supporting online material.
20. D. W. Bierhorst, On the stem apex, leaf initiation and early leaf ontogeny in filicalean ferns. *Am. J. Bot.* **64**, 125 (1977). [doi:10.2307/2442101](https://doi.org/10.2307/2442101)
21. C. J. Harrison, A. H. K. Roeder, E. M. Meyerowitz, J. A. Langdale, Local cues and asymmetric cell divisions underpin body plan transitions in the moss *Physcomitrella patens*. *Curr. Biol.* **19**, 461 (2009).  
[doi:10.1016/j.cub.2009.02.050](https://doi.org/10.1016/j.cub.2009.02.050) [Medline](#)
22. J. Luck, H. B. Luck, Plant cell assemblage in layers. *Acta Biotheor.* **43**, 95 (1995).  
[doi:10.1007/BF00709436](https://doi.org/10.1007/BF00709436)
23. S. E. Siegrist, C. Q. Doe, Microtubule-induced Pins/Galphai cortical polarity in *Drosophila* neuroblasts. *Cell* **123**, 1323 (2005). [doi:10.1016/j.cell.2005.09.043](https://doi.org/10.1016/j.cell.2005.09.043)  
[Medline](#)
24. J. Voog, C. D'Alterio, D. L. Jones, Multipotent somatic stem cells contribute to the stem cell niche in the *Drosophila* testis. *Nature* **454**, 1132 (2008).  
[doi:10.1038/nature07173](https://doi.org/10.1038/nature07173) [Medline](#)
25. T. Sato *et al.*, Single Lgr stem cells build crypt-villus structures in vitro without a mesenchymal niche. *Nature* **459**, 262 (2009).
26. S. R. Cutler, D. W. Ehrhardt, J. S. Griffiths, C. R. Somerville, Random GFP:cDNA fusions enable visualization of subcellular structures in cells of *Arabidopsis* at a high frequency. *Proc. Natl. Acad. Sci. U.S.A.* **97**, 3718 (2000). [doi:10.1073/pnas.97.7.3718](https://doi.org/10.1073/pnas.97.7.3718) [Medline](#)
27. B. K. Nelson, X. Cai, A. Nebenführ, A multicolored set of in vivo organelle markers for co-localization studies in *Arabidopsis* and other plants. *Plant J.* **51**, 1126 (2007). [doi:10.1111/j.1365-313X.2007.03212.x](https://doi.org/10.1111/j.1365-313X.2007.03212.x) [Medline](#)

28. T. Murashige, F. Skoog, A revised medium for rapid growth and biol. assays with tobacco tissue cultures. *Physiol. Plant.* **15**, 473 (1962). [doi:10.1111/j.1399-3054.1962.tb08052.x](https://doi.org/10.1111/j.1399-3054.1962.tb08052.x)
29. <http://cmpdartsvr1.cmp.uea.ac.uk/wiki/BanghamLab/index.php/BioformatsConverter>.
30. M. D. Abramoff, P. J. Magelhaes, S. J. Ram, Image Processing with ImageJ. *Biophotonics Int.* **11**, 36 (2004).
31. P. Barbier de Reuille, I. Bohn-Courseau, C. Godin, J. Traas, A protocol to analyse cellular dynamics during plant development. *Plant J.* **44**, 1045 (2005). [doi:10.1111/j.1365-313X.2005.02576.x](https://doi.org/10.1111/j.1365-313X.2005.02576.x) [Medline](#)
32. C. Smith, P. Prusinkiewicz, F. Samavati, Local specification of surface subdivision algorithms (Applications of Graph Transformations with Industrial Relevance (AGTIVE 2003)). *Lect. Notes Comput. Sci.* **3062**, 313 (2003). [doi:10.1007/978-3-540-25959-6\\_23](https://doi.org/10.1007/978-3-540-25959-6_23)